Mechanical Characterisation of Multi-Wythe Masonry Bridge in the City of Amsterdam

Xi Li, Francesco Messali, and Rita Esposito(✉)

Faculty of Civil Engineering and Geosciences, Delft University of Technology, Stevinweg 1, 2628CN Delft, The Netherlands
{xi.li,f.messali,r.esposito}@tudelft.nl

Abstract. This paper presents the results of an experimental campaign carried out to characterise the mechanical properties of multi-wythe masonry infrastructure in the city of Amsterdam. Samples were extracted from a 1.2 m thick bridge's pillar constructed in 1882. For the characterisation of shear and compressive properties of masonry, tests on cores with a 100 mm diameter were performed at the Stevin-laboratorium of Delft University of Technology. Samples were extracted along different locations in the wall thickness to evaluate the effect of exposure to environment conditions. Overall, the study provides a first insight on the mechanical properties of multi-wythe masonry city infrastructure and knowledge regarding the sampling and testing strategy for these structures. In turn, this will increase the knowledge on multi-wythe masonry, which is limited in literature, and will support the assessment of many infrastructures in typical Dutch canal cities.

Keywords: masonry · cylindrical cores · slightly-destructive testing method · nonlinear shear-sliding behaviour · nonlinear compressive behaviour · Dutch city infrastructure

1 Introduction

Over 200 km of quay walls and several bridges are in urgent need of renovation in the city of Amsterdam [1]. Nowadays, masonry structures do not only represent an important infrastructure for the viability of the city, but they are also important historical assets. In recent years, brides and quay walls showed substantial deformation and in some cases even collapse, e.g. [2]. Pillars and abutment of bridges and well as quay walls are often made of multi-wythe masonry with a thickness of more than 600 mm. Not much is known about the mechanical characterisation of these URM structures, thus reducing the reliability of their structural assessment and renovation. Numerical models that are used for the structural assessment require the definition of material parameters based on the nonlinear behaviour of masonry and its constitutes (i.e. brick and mortar) under various loading conditions like compression, shear, bending, etc. [3]. Therefore, it is necessary to perform experimental tests on these old masonry structures, to characterise their mechanical properties and to provide the definition of input parameters for nonlinear finite element analyses.

Y. Endo and T. Hanazato (Eds.): SAHC 2023, RILEM Bookseries 47, pp. 527–540, 2024.
https://doi.org/10.1007/978-3-031-39603-8_43

Regarding testing methods, core testing on small-diameter cylindrical samples has shown the great potential for existing and historical masonry structures due to their slightly-destructive nature [4–6]. It allows testing the samples in laboratory with standard set-up and granting the possibility of acquiring the post-peak softening of masonry under shear and compressive loadings. Both shear properties at brick-mortar interfaces and compressive properties of single-wythe masonry can be successfully obtained by small-diameter cores. To characterise shear properties, splitting tests are usually performed on I-shaped cores with one bed joint rotated at different inclination angles [5, 7–9]. Mazzotti et al. [7] investigated the effect of inclination angles of 0°, 15°, 30°, 40°, 45° and 50° on the failure modes of cores. They conclude that cores with angles between 15° and 30° exhibited a splitting failure mode, while cores with a higher mortar joint inclination exhibited a sliding failure mode. For evaluating masonry shear resistance, sliding failure mode is generally considered as the most representative failure mode, thus high inclination angles around 40°−50° are recommended. Jafari et al. [5] compared shear properties obtained from splitting tests on I-shaped cores (one bed joint) and shear-compression tests on triplets for various masonry types; she found a correlation coefficient 0.88 for initial shear strength and 0.96 for friction coefficient. As for the compressive properties, cores with different diameters, thickness and bond patterns can be found in literature [4, 6, 10]. Segura et al. [10] explored the size effect on the compressive behaviour obtaining that the compressive strength and the Young's modulus were, respectively, 25% and 15% higher for I-shaped cores with a diameter of 90 mm with respect to H-shaped cores with a diameter of 150 mm (two bed joints and one head joint). Conversely, Jafari et al. [6] did not find substantial difference in results by testing T-shaped cores with a diameter of 100 mm (one bed joints and one head joint) and H-shaped cores with a diameter of 100 mm; additionally, she found a 1:1 correlation factor with tests on wallets. Overall, the core testing method can be regarded as a reliable alternative to conventional standardized methods.

Currently, research on mechanical properties of multi-wythe masonry structures is limited in literature, especially the material characterisation with the consideration of through-thickness effect, namely potential variation of mechanical properties in the wall thickness due to different environmental conditions. Some work can be found at the structural level. Isfeld et al. [11] studied the effect of grout injection, as an effective repair method, on the deformation of stone masonry walls. Sortour et al. [12] designed in-plane and out-of-plane testing programs to determine the elastic and shear moduli of masonry wall with a dimension of $2 \times 2.75 \times 0.54$ m^3 (width × height × thickness). In terms of material characterisation, Demir and Ilki [13] compared the damage evolution and material properties of multi-wythe and single-wythe masonry prisms under compression. In comparison with single-wythe prisms, they found that: i) multi-wythe prisms present vertical cracks along the interfaces of the external and internal wythe at earlier steps of the loading; ii) the overall axial deformability was significantly higher and the compressive strength was almost halved. Until now, we are still lack of a comprehensive understanding about material characterisation of multi-wythe masonry walls under various loading conditions like shear, compression, bending. Therefore, an experimental strategy for the evaluation of such thick structure is urgently needed.

To provide insights on how to characterise multi-wythe masonry infrastructure, a pilot study has been started at Delft University of Technology in 2022 with the characterisation of a bridge's pillar built in 1882 in Amsterdam. Various mechanical tests, including tests on cores and on standard rectangular samples (e.g. couplets, prisms, triplets) were performed. In this paper, the outcome of core tests to characterise shear and compressive properties of masonry are presented and discussed. Splitting tests and compressive tests were performed on I-shaped cores (one bed joint) and T-shaped cores (one head joint and one bed joint), respectively, both with a diameter of 100 mm. Samples were extracted in the portion of masonry above water level and different samples through the thickness direction of the masonry wall were collected. The scope of this paper is to discuss the suitability of the core testing method for to multi-wythe masonry in city infrastructure exploring the effect of exposure to environmental conditions on mechanical properties.

2 Material and Methods

2.1 Material and Sample Extraction Process

During the renovation of a bridge in Amsterdam (the Netherlands), a portion of masonry with dimensions $0.6 \times 1.4 \times 1.2$ m^3 (length $\times$ height $\times$ thickness) was extracted from a pillar originally built in 1882. The extraction took place in April 2020; afterwards the portion was caged in a steel box and stored. The portion of masonry was made of solid clay bricks having on average a length of 210 mm, a height of 50 mm and a thickness of 100 mm, and of the mortar joints having a thickness ranging between 2–20 mm. Regarding the bond pattern, the front side of the masonry wall was built in Dutch bond (a row of headers alternated to a row of stretchers). However, through the thickness direction the bricks were mainly laid as headers although a clear bond pattern was not identified.

The extraction of sample for material characterisation took place in 2022 and the procedure consisted of two phases. In the first phase, the masonry portion was sawed along the thickness using diamond blades, so that 6 pieces (Piece 1–6) were obtained with average dimensions of $600 \times 1200 \times 210$ mm3 (see Fig. 1(a)). In the second phase, a wet extraction procedure was employed to drill I-shaped and T-shaped cores with a diameter of 100 mm and a thickness of approximately 100 mm from Piece 1–4, for the splitting tests and compressive tests, respectively. Figure 1(b) shows one of the sawed masonry pieces after the wet drilling process of cores from the front view.

Considering a possible variation of the properties based on the exposure conditions (e.g. close to or far of water), it was assumed that three masonry objects could exist: an external one (Piece 1 and 6), a middle one (Piece 2 and 5), and internal one (Piece 3–4). A masonry object is identified as masonry of the same typology subject to the same exposure condition. A masonry typology is a masonry made of the same bricks and mortar type and built in a specific time.

2.2 Testing Set-Ups and Procedures

Splitting tests on I-shaped cores were carried out inclining the mortar bed joint at 45°, 50° and 55° with respect to its original position. The test allows inducing a mixed

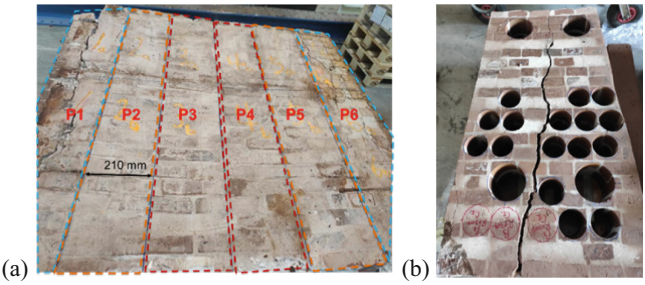

(a) (b)

Fig. 1. Sampling: (a) Sawing plan through-thickness view; (b) Sawed masonry piece after the wet extraction of cores.

compression-shear stress state at the centre of the mortar joint, as shown in Fig. 2(a). The test was carried out by a sliding-controlled apparatus including a hydraulic jack with 100 kN capacity (see Fig. 2(b)-(c)). Two wooden strips, with dimension of 194 × 15 × 2 mm, were inserted between the loading plates and the sample to distribute the load. The relative sliding displacement and normal displacement between the two bricks was measured using two LVDTs on each face of the specimen. The LVDTs have a measuring range of 2 mm. The average sliding measurements (between front and back face) was used to control the load. A sliding-displacement-rate of 0.1 μm/s was adopted during the tests. At least three samples were tested for each inclination.

Compression tests were carried out on T-shaped cores with a diameter of 100 mm by using a high-strength mortar cap (Fig. 3). Due to the unpredictable bond in the thickness of the pillar, the core had a thickness ranging between 65 and 100 mm to avoid the presence of any collar joint in the specimen. Wooden moulds with a dimension of 70 × 100 × 50 mm were designed to assist the capping process, as showed in Fig. 3 (a). If cores were slightly shorter than the mould length, clay mould and polystyrene material were used to fill the mould. The high strength mortar named "Cement Cuglaton Gietmortel 1 mm" was used by mixing of 0.75 kg water per 5 kg. The mortar had a mean flexural strength of 5.5 MPa and mean compressive strength of 61.37 MPa after 7 days of curing at room temperature (EN 1015–11 [14]). After casting the mortar, the mould was covered with a plastic sheet. De-moulding occurred after 1 day from casting. After 7 days of curing at room temperature, the samples were tested (see Fig. 3 (b)). The samples were instrumented with four LVDTs at the front and back sides (Fig. 3 (c)). Two vertical LVDTs with a measuring range of 10 mm were glued to the brick approximately at the centre of the specimen's face. Two horizontal LVDTs with a measurement range of 2 mm were attached to brick along the horizontal axis. The test was carried out using a displacement-controlled set-up to explore the post-peak behaviour. A testing machine including a hydraulic jack with 3500 kN capacity was used. A displacement rate of 0.002 mm/s was adopted. The compression test was performed monotonically. Four to five specimens from Piece 1–3 were tested, while only two specimens from Piece 4 were tested as few T-shaped cores were founded during the extraction.

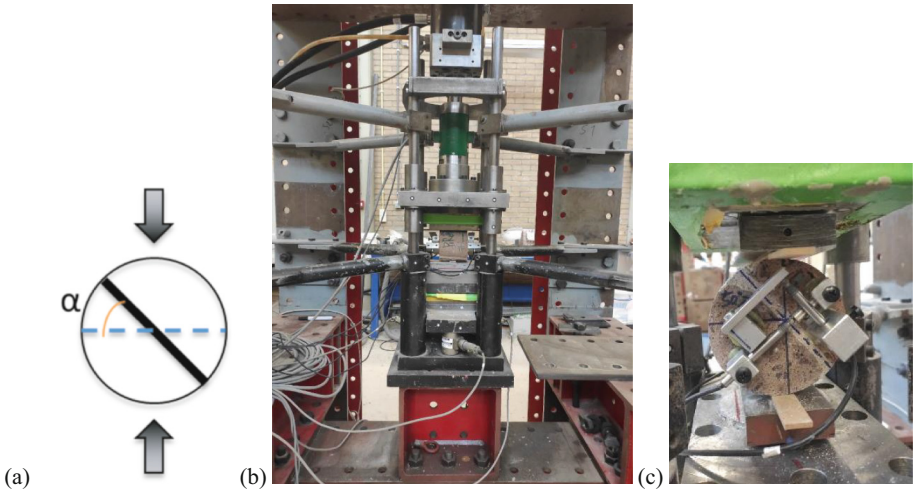

Fig. 2. Splitting test on core: (a) Definition of inclination angle α; (b) Splitting test set-up; (c) Measurement system.

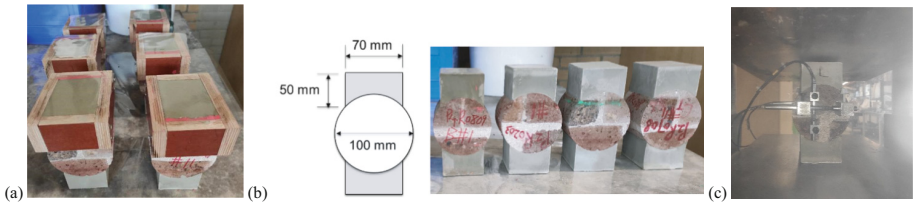

Fig. 3. Compression tests on core: (a) Capping process using wooden moulds; (b) Specimen's geometry; (c) Test set-up.

3 Mechanical Characterisation with Core Testing

3.1 Shear Properties

The normal stress at failure and the shear strength were determined as:

$$f_{p,core} = \frac{F_{max}}{A} \cos \alpha \tag{1}$$

$$f_{v,core} = \frac{F_{max}}{A} \sin \alpha \tag{2}$$

where F_{max} is the maximum force from the testing machine, A is the area of the mortar layer, and α is the mortar layer inclination, with respect to the horizontal reference.

By considering the Coulomb friction criterion, the value of the initial shear strength $f_{v0,core}$ and the coefficient of friction μ_{core} were evaluated by a linear regression of the shear and compressive stresses obtained by tests on cores with different mortar layer inclinations. In literature, two methods are reported for the evaluation of the shear

properties of masonry: the linear regression considering the average strength per each mortar inclination (as proposed by Mazzotti et al. [7] and adopted by Jafari et al. [5]), or the linear regression of all the data (as proposed by Pelà et al. [8]). In the present work, both methods are applied for comparison.

The following four types of failure modes are usually observed in splitting tests on I-shaped cores:

- Sliding along one brick-mortar interface (Fig. 4(a)).
- Sliding along two brick-mortar interfaces including mortar failure (Fig. 4 (b)).
- Mixed sliding-tensile failure with cracks mainly at interfaces and few cracks in bricks (Fig. 4 (c)).
- Tensile failure with a vertical crack parallel to the loading direction located in the middle of the core (Fig. 4 (d)).

In the present study, the majority of cores failed in the mixed sliding-tensile failure mode (Fig. 4 (c)), while the rest failed in the tensile failure mode (Fig. 4 (d)). To calculate the shear properties at brick-mortar interface, only the former have been considered. Table 1 lists the number of samples with mixed sliding-tensile failure involved in the data analysis.

Figure 5 shows the force versus the sliding displacement measured between the two portions of bricks for cores listed in Table 1. Each colour of line plots in Fig. 5 represents samples from each wall piece. As the testing machine was controlled by the sliding displacement measured by LVDTs, the post-peak behaviour was recorded for all samples. Not significant through-thickness effect can be observed on the relation of sliding displacement and shear stress among cores extracted from Piece 1 to Piece 4. However, this conclusion should be taken with care because the experimental results are limited and show a high coefficient of variation.

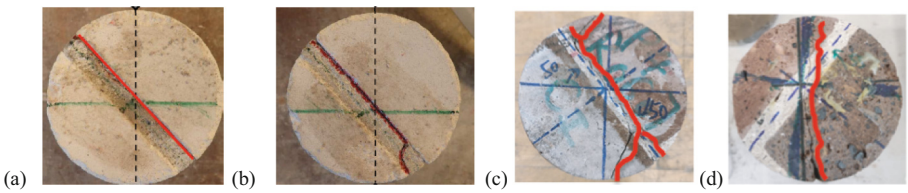

Fig. 4. Typical failure mode of cores after splitting tests (a) Sliding along one brick-mortar interface [5]; (b) Sliding along two brick-mortar interfaces [5]; (c) Mixed sliding-tensile failure; (d) Tensile failure.

Figure 6 shows the failure envelope in terms of shear stress versus compression stress relationship for all the results obtained from Piece 1 to 4. Considering the regression analysis with the average results for each inclination [7], an initial shear strength f_{V0} of 1.13 MPa and coefficient of friction μ of 0.17 are obtained (Fig. 6 (a)); however, these results are unconventional considering typical values for brick masonry [5, 7, 8]. Considering the regression analysis of all results [8], an initial shear strength f_{V0} of 0.51 MPa and coefficient of friction μ of 0.83 are obtained (see Fig. 6 (b)), which are

Table 1. Number of cores tested at each inclined angle with mixed sliding-tensile failure.

Inclined angle Wall portion	45º	50º	55º
Piece 1	0	0	1
Piece 2	2	1	2
Piece 3	1	1	2
Piece 4	3	2	3
Total number of samples	6	4	8

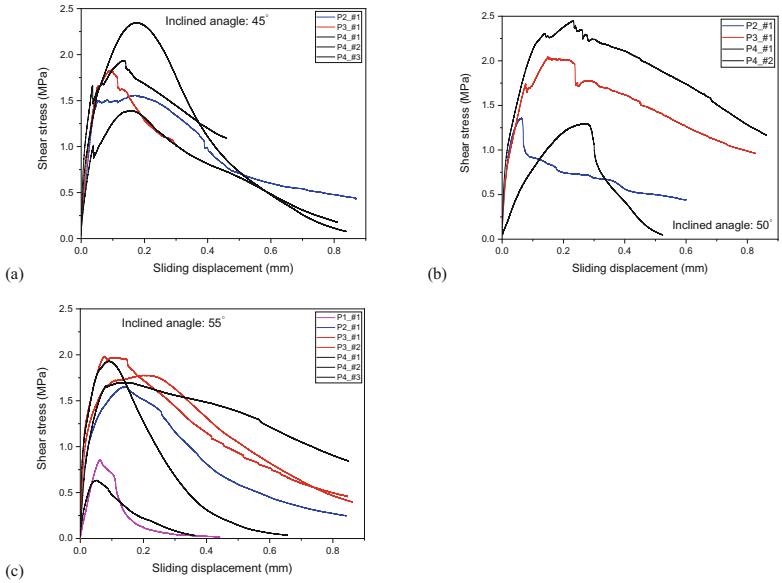

Fig. 5. Shear stress versus joint relative displacement for different mortar layer inclinations: (a) $\alpha = 45º$; (b) $\alpha = 50º$; (c) $\alpha = 55º$.

within the scatter range of what reported in literature [5, 7, 8]. Considering the large scatter of the results, the latter method seems to be more appropriate for this case study.

To provide an estimate of the dissipated energy, fracture energy under shear is calculated by using the method proposed by Jafari et al. [5] (Fig. 7) where the fracture energy due to friction at interfaces was excluded. The stress component due to friction is computed as the normal stress multiplying by the coefficient of friction from Fig. 6 (b) and it varies during the splitting tests of cores (see the blue line in Fig. 7). The fracture energy under shear from cores of Piece 1–4 ranges from 42.89 to 1591.1 N/m. Most of values are higher than what obtained in previous research [5], indicating that the energy dissipated in the partial failure of the brick is not negligible. This may indicate that the bond at the interface and the strength of brick and mortar is of a better quality than

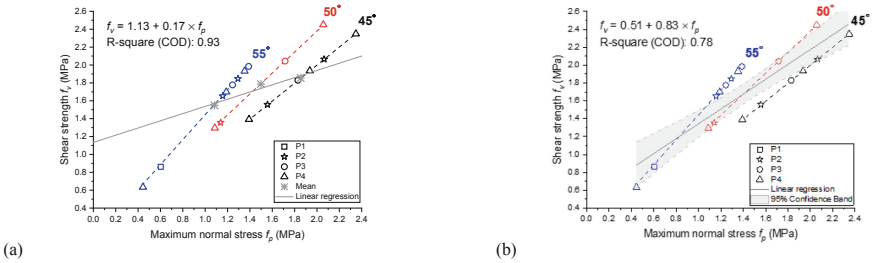

Fig. 6. Failure envelope from splitting tests on cores using: (a) the average result for each inclination; (b) all data.

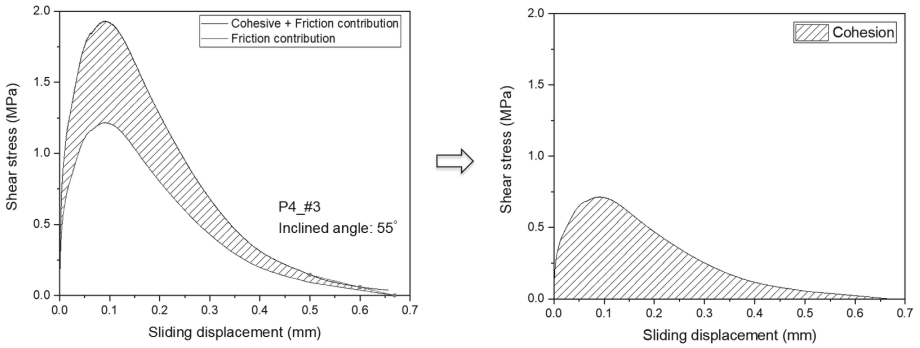

Fig. 7. Calculation of fracture energy from shear stress-sliding curves according to Jafari et al. [5].

masonry extracted from buildings (which was mainly the object of previous studies with core testing method). Nevertheless, it also suggests that improvements to the testing method to take these factors into account are actually needed.

3.2 Compressive Properties

The following compressive properties were evaluated from the core testing: Young's modulus, compressive strength and corresponding peak strain, and compressive fracture energy.

The compressive strength of masonry core can be calculated either by considering the cross-section of the core or the cross-section of the cap, as suggested by Pelà et al. [4]. In this paper, following Jafari et al. [5], the cross-section of the cap is used to evaluate the stress state:

$$f'_{m,core} = \frac{F_{max}}{B_{cap} L_{cap}} \tag{3}$$

where F_{max} is the maximum load, B_{cap} is the width of the cap (along the face of the core), and L_{cap} is the length of the cap (along the thickness of the core). The strain corresponding

to the compressive strength is defined as the peak strain. For the elastic modulus, the chord Young's modulus E evaluated between 1/10 and 1/3 of the maximum stress is adopted. The displacement control procedure of the test allows determining the post-peak behaviour of the material. The fracture energy in compression $G_{f\text{-}c}$ was determined as the area underneath the normal stress versus normal strain diagram, taking the height of the specimen into account. This concept was introduced by van Mier [15] for concrete material and subsequently applied to masonry by Lourenço [16].

As shown in Fig. 8 (a), the strain obtained by LVDTs' readings and by the jack's readings resulted similar in the post-peak phase. Consequently, the former were used to evaluate the properties in the pre-peak phase, while the latter were used to describe the post-peak phase, in which LVDTs were detached from the specimen due to extensive cracking. Consequently, the displacements measured from the jack were shifted to define the post-peak stress-strain relationship curve (see Fig. 8 (a)), as proposed by Jafari et al. [6]. The elastic modulus was calculated based on the LVDTs readings, while the fracture energy was calculated based on the LVDTs' reading in the pre-peak and modified jack's reading in the post-peak phase. The ultimate displacement was obtained by prolonging a linear curve from the "shifted" stress-strain curve from jack measurements; the slope of this linear curve was defined based on axial stress - axial displacement relation near the end of testing (see Fig. 8 (b)).

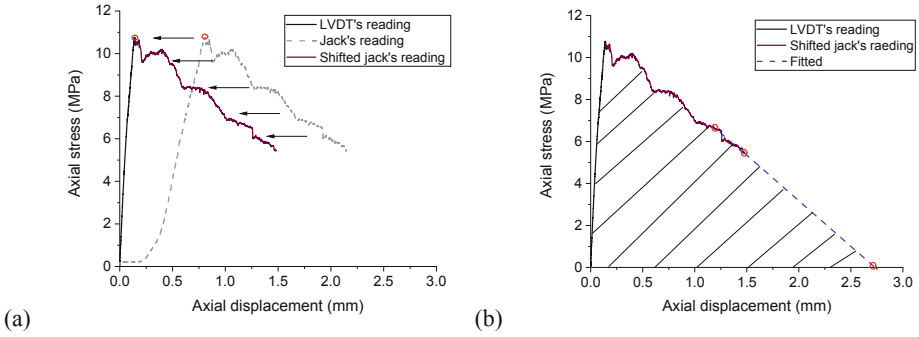

Fig. 8. (a) Capturing the full response under compression loading using LVDTs' readings in the pre-peak and jack's readings in the post-peak phase; (b) Estimation of compressive fracture energy.

Figure 9 shows the typical crack evolution in T-shaped cores. For most cases, at the first reduction of stress, the crack occurred suddenly along the head joint of the cores and propagated to the cap (Fig. 9(a)). With the increase of the axial strain, the crack opened perpendicular to the loading direction and propagated vertically (Fig. 9(b)). After the peak stress, multiple cracks generated broadly and led to the final collapse (Fig. 9(c)). The premature failure of the cap was undesired, but it could not be associated to any geometrical imperfection. Considering the rapid recover of stresses after onset of cracking, it can be considered that this premature failure has a negligible influence on the compressive strength and peak strain; on the other hand results associated to the fracture energy should be taken with care.

Figure 10 shows the axial stress versus the axial strain obtained from both LVDTs and jack measurements for T-shaped cores extracted from Piece 1 to Piece 4. Due to the detachment of LVDTs, the post-peak behaviour of some specimens are missing in Fig. 10 (a). For all the samples, the stress-strain response under compression starts from a linear-elastic stage, which is then followed by an hardening behaviour until the peak stress. This hardening stage usually initiates at the first reduction of force during the testing. After reaching the peak stress, both nonlinear and linear softening behaviour can be observed for different specimens. The slope of the stress-strain curves in the linear-elastic stage is steeper for samples from Piece 1 and Piece 2 (external), than those from Piece 3 and Piece 4 (internal). Subsequently, a lower peak strain is recorded for specimens from Piece 1 and Piece 2, in comparison with the specimens from Piece 3 and Piece 4.

Figure 11 shows the mean values of compressive properties for each piece. As observed, the compressive strength and compressive fracture energy are similar through the thickness direction of the masonry wall, with a mean value of 12.36 MPa and 19.40 N/mm (see the dash line in Fig. 11 (a) and (c)), respectively. In Fig. 11 (b) and (d), a decreasing trend of the elastic modulus and an increasing trend of the peak strain are presented for specimens from the near-water side to the internal region of the pillar. This phenomenon indicates that the compressive behaviour of the masonry becomes more brittle when being closer to water. This may be due to geometrical properties of the specimen, i.e. large variation in the joint's thickness, or suggest the presence of degradation mechanisms.

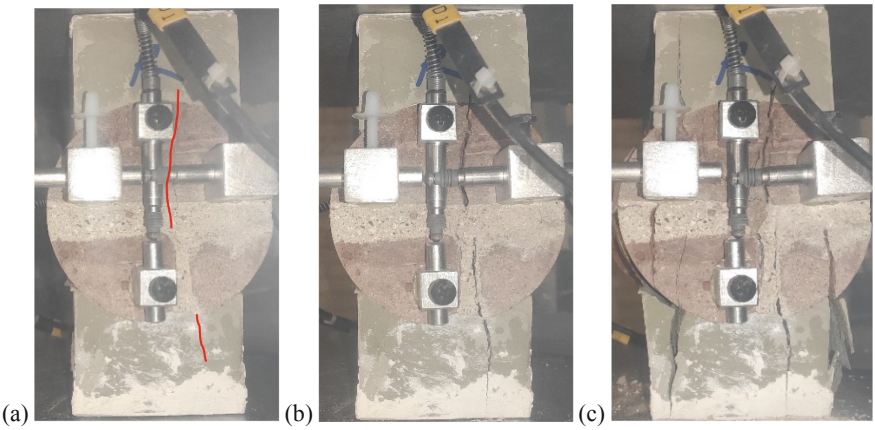

Fig. 9. Typical crack pattern in compression tests on T-shaped cores: (a) onset of cracking, (b) peak stress, (c) end of the test.

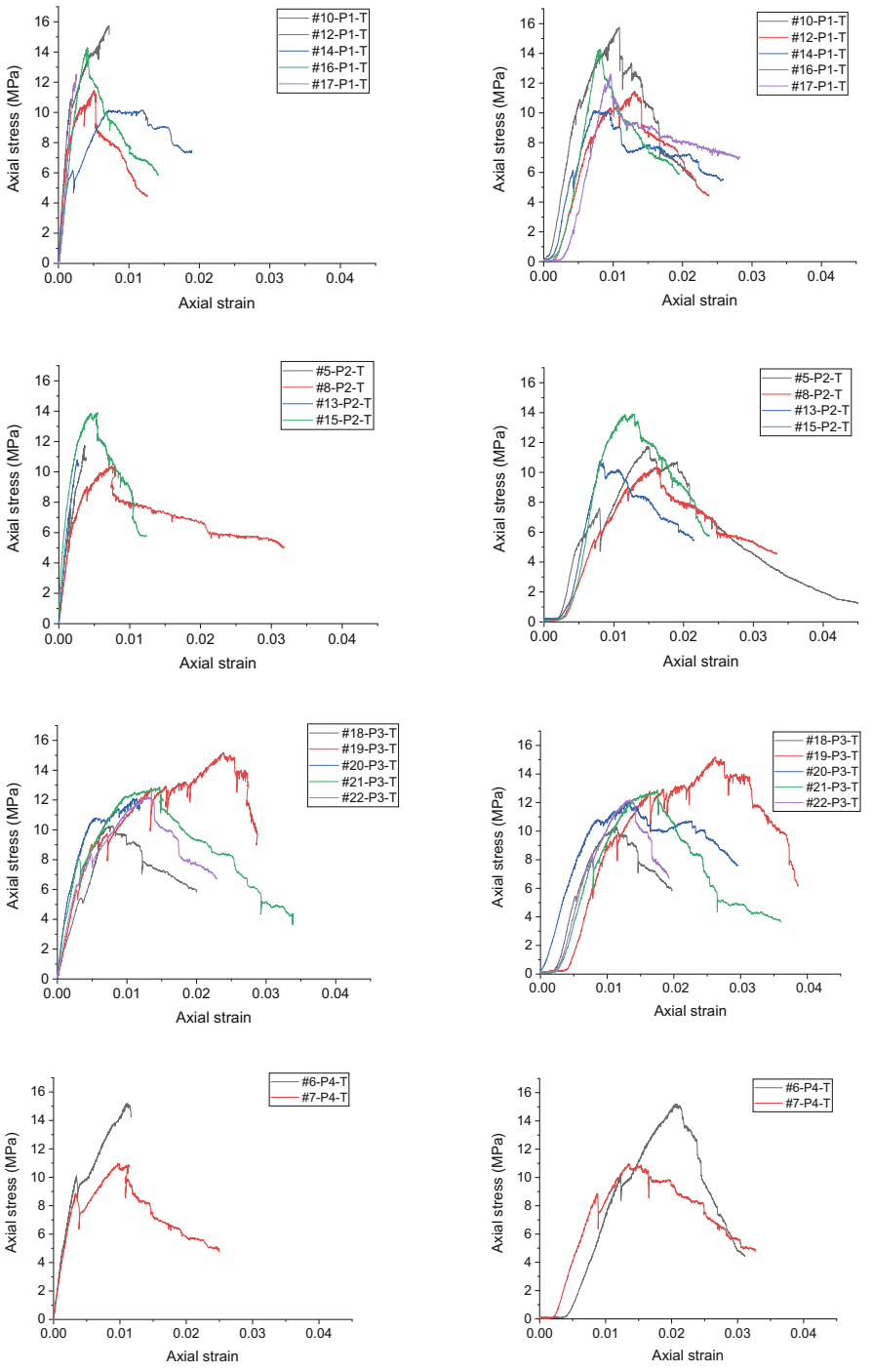

Fig. 10. Compression behaviour of T-shaped cores from Piece 1 to 4: (a) normal strain obtained by LVDT's reading; (b) normal strain obtained by jack's reading.

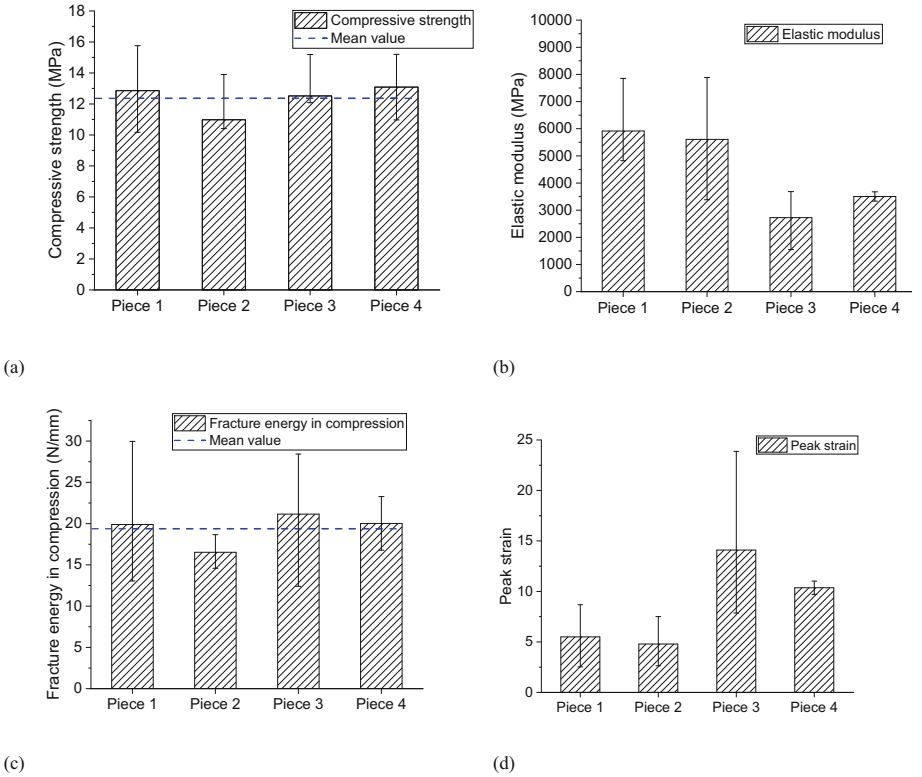

Fig. 11. Mean value of compressive properties for each Piece (Piece 1 external, Piece 4 internal): (a) Compressive strength (b) Elastic modulus (c) Fracture energy in compression (d) Peak strain.

4 Conclusions

Based on the analysis of splitting tests of I-shaped cores and compressive tests of T-shaped cores extracted from an old bridge pillar, the present work provides preliminary conclusions for the characterisation of typical Dutch city infrastructures:

- Due to the difficulties of extracting standard rectangular samples from multi-wythe masonry infrastructure, the core testing method seems to be one of the most efficient slightly-destructive test to be employed for characterisation of mechanical properties. Additionally, this gives the advantage that in case of composite structures, i.e. masonry-concrete walls, the same sample can be adopted independently of the construction material.
- Due to significant scatter of test data for the splitting tests, for the calculation of shear properties (i.e. initial shear strength and coefficient of friction) the regression line approximating all the data is more reliable than that approximating the average of each inclination. Nevertheless, further investigations are needed to evaluate the role of brick failure in the mixed tensile-sliding failure mode.

- For this case study, it was not possible to evaluate the through-thickness effect on the shear properties, due to the limited data and the high coefficient of variation. On the contrary, a through-thickness effect for some compressive properties could be identified.
- The stress-strain curves showed that compressive behaviour of the masonry is more brittle when being closer to water.
- For this case study, the through-thickness effect on the compressive behaviour seems to be different for different properties. The compressive strength and compressive fracture energy are similar among different pieces of the masonry wall. Conversely, the elastic modulus and peak strain show, respectively, a decrease and an increase when moving from the water side towards the inner side of the wall. This may due to geometrical properties of the specimen, i.e. large variation in the joint's thickness, or suggest the presence of degradation mechanisms.

To further understand and interpret the results of the splitting tests on cores, further tests are planned to be conducted including shear-compression tests on triplets, bond wrench tests on couplets and flexural tests on bricks. In addition, experimental campaigns on rectangular samples are needed to correlate the compressive properties from cores to standard samples like wallets or prisms. In turn, this aim at defining a strategy for the mechanical characterisation of multi-wythe masonry, which is limited in literature, and will support the assessment of many infrastructure in typical Dutch canal cities.

Acknowledgements. This research was funded by the municipality of Amsterdam via the Amsterdam institute for Advanced Metropolitan Solutions (AMS) within the scope of the research programme Bridges and Quay Walls (Programma Bruggen en Kademuren).

References

1. Kademuren. maatregelen en vernieuwen [Internet] (2022). Available from: https://www.amsterdam.nl/projecten/kademuren/
2. Korff, M., Hemel, M., Esposito, R.: Bezwijken Grimburgwal: Leerpunten voor het Amsterdamse areaal. Delft, The Netherlands (2021)
3. Sharma, S., Longo, M., Esposito, R., Messali, F.: Structural assessment of a masonry quay wall in Amsterdam under traffic loading. In: Kyoto (Japan): 26th International Conference on Structural Analysis of Historical Constructions (SAHC) (2023)
4. Pelà, L., Canella, E., Aprile, A., Roca, P.: Compression test of masonry core samples extracted from existing brickwork. Constr. Build. Mater. **119**, 230–240 (2016)
5. Jafari, S., Rots, J.G., Esposito, R.: Core testing method to assess nonlinear shear-sliding behaviour of brick-mortar interfaces: a comparative experimental study. Constr. Build. Mater. **244**, 118236 (2020)
6. Jafari, S., Rots, J.G., Esposito, R.: Core testing method to assess nonlinear behavior of brick masonry under compression: a comparative experimental study. Constr. Build. Mater. **218**, 193–205 (2019)
7. Mazzotti, C., Sassoni, E., Pagliai, G.: Determination of shear strength of historic masonries by moderately destructive testing of masonry cores. Constr. Build. Mater. **54**, 421–431 (2014)
8. Pelà, L., Kasioumi, K., Roca, P.: Experimental evaluation of the shear strength of aerial lime mortar brickwork by standard tests on triplets and non-standard tests on core samples. Eng. Struct. **136**, 441–453 (2017)

9. Marastoni, D., Pelà, L., Benedetti, A., Roca, P.: Combining Brazilian tests on masonry cores and double punch tests for the mechanical characterization of historical mortars. Constr. Build. Mater. 112, 112–27 (2016). [Internet]. Available from: https://doi.org/10.1016/j.conbuildmat.2016.02.168
10. Segura, J., Pelà, L., Roca, P., Cabané, A.: Experimental analysis of the size effect on the compressive behaviour of cylindrical samples core-drilled from existing brick masonry. Constr. Build. Mater. **228**, 116759 (2019)
11. Isfeld, A.C., Moradabadi, E., Laefer, D.F., Shrive, N.G.: Uncertainty analysis of the effect of grout injection on the deformation of multi-wythe stone masonry walls. Constr. Build. Mater. **126**, 661–672 (2016)
12. Sorour, M., Elmenshawi, A., Parsekian, G., Mufti, A., Jaeger, L.G., Duchesne, D.P.J., et al.: An experimental programme for determining the characteristics of stone masonry walls. Can. J. Civ. Eng. **38**(11), 1204–1215 (2011)
13. Demir, C., Ilki, A.: Characterization of the materials used in the multi-leaf masonry walls of monumental structures in Istanbul. Turkey. Constr. Build. Mater. **64**, 398–413 (2014)
14. NEN-EN 1015–11. Methods of test for mortar for masonry - Part 11: Determination of flexural and compressive strength of hardened (2019)
15. Van Mier, J.G.M.: Strain-softening of concrete under multiaxial loading conditions, pp. 1–244 (1984)
16. Lourenço, P.B., De Borst, R., Rots, J.G.: A plane stress softening plasticity model for orthotropic materials. Int. J. Numer. Meth. Eng. **40**(21), 4033–4057 (1997)
17. Author, F., Author, S., Author, T.: Book title. 2nd edn. Publisher, Location (1999)
18. Author, F.: Contribution title. In: 9th International Proceedings on Proceedings, pp. 1–2. Publisher, Location (2010)
19. LNCS Homepage, http://www.springer.com/lncs. Last accessed 21 Nov 2016